Quantum optics of traveling-wave attenuators and amplifiers

J. R. Jeffers*

Physics Department, Essex University, Colchester CO4 3SQ, England

N. Imoto

NTT Basic Research Laboratories, 3-9-11 Midori-cho, Musashino-shi, Tokyo 180, Japan

R. Loudon

Physics Department, Essex University, Colchester CO4 3SQ, England

We use a continuous-mode quantization scheme to derive relations between the output- and input-field operators for traveling-wave propagation along attenuating and amplifying optical fibers. These relations provide complete information on the temporal and longitudinal spatial developments of the signal field. They are used here to obtain the effects of propagation on the first and second moments of the photocount in direct detection and of the signal field measured in balanced homodyne detection. Some of the results are similar to those obtained for attenuation or amplification of standing waves in cavities, and, for example, the survival of any input squeezing still limits the maximum gain to twofold. There are, however, additional propagation effects for the traveling-wave system. Thus, in direct detection, it is necessary to take account of the changes in gain profile with propagation distance, and in homodyne detection there are fundamental quantum-mechanical restrictions on the minimum field uncertainties that can be achieved in measurements at separated space-time points. These uncertainty properties are derived in detail and illustrated by the example of a squeezed input signal.

PACS number(s): 42.50.Lc, 42.50.Dv, 42.81.Dp

I. INTRODUCTION

There is much current interest in the generation of light beams whose measured noise levels lie below those allowed by the semiclassical theory of photodetection [1]. Such nonclassical light may have important applications in low-noise measurement and communication systems, where the effects of optical processing on the nonclassical properties can only be understood within the framework of quantum optics. Thus in optical communications with nonclassical input light, it is necessary to use the quantum theory to determine the effects of propagation along lossy or amplifying fibers on the initially reduced noise.

The quantum theory of light has traditionally been formulated in terms of the discrete standing-wave modes of the electromagnetic field confined within an optical cavity [2]. This quantization scheme is, however, awkward to apply to traveling-wave propagation along an optical fiber, where the beam properties vary with distance, in addition to the time dependences associated with the information carried by the beam. The cavity-quantization theory can easily handle only the time dependence of an optical field, and it also suffers from the lack of any readily identifiable cavity in most traveling-wave systems, where the optical energy flows from sources to detectors with no significant reflection or recycling. These difficulties have stimulated the development of cavity-free continuous-mode quantization schemes [3–5] that are better suited to the treatment of traveling-wave problems.

Optical fibers are made from dispersive materials with frequency-dependent refractive indices $\eta(\omega)$. There has been much recent work on the quantization of the electromagnetic field in such media and on the resulting dielectric effects on the quantum properties of light [5–12]. The form of the positive-frequency part of the electric-field operator appropriate to propagation along an optical fiber of effective cross-sectional area A is

$$\hat{E}^+(z,t) = i \int_0^\infty d\omega \left[\frac{\hbar\omega}{4\pi\epsilon_0 c A \eta(\omega)} \right]^{1/2} \hat{a}(\omega)$$
$$\times \exp\left\{ -i\omega\left[t - \frac{\eta(\omega)z}{c} \right] \right\}, \qquad (1.1)$$

where the creation and destruction operators of the one-dimensional continuum of modes of frequency ω satisfy the usual commutator

$$[\hat{a}(\omega), \hat{a}^\dagger(\omega')] = \delta(\omega - \omega') . \qquad (1.2)$$

The purpose of the present paper is the application of these quantization methods, particularly in the form described by Blow *et al.* [5], to the quantum optics of traveling-wave attenuators and amplifiers (brief preliminary accounts of the work are given in Refs. [13] and [14]). Previous work has treated the traveling-wave phase-sensitive degenerate parametric amplifier [3,15,16], and there is also existing theoretical and experimental work on phase-insensitive amplifiers, for example, rare-earth-doped fiber amplifiers [17] and Raman amplifiers [18]. Our aim here is to give more comprehensive treat-

ments of traveling-wave phase-insensitive attenuation and amplification. We pay particular attention to the field properties that can be measured by direct and by homodyne detection. In the latter case we derive uncertainty relations for the homodyne noise in measurements made at different propagation distances, and we show how the minimum noise conditions can be realized for a squeezed-light input signal. The effect of propagation along a gain-compensated low-loss fiber on the noise level of initially squeezed light is determined.

It is usually the case that the signal bandwidth B is much smaller than its central frequency ω_0. Furthermore, for weakly amplifying fibers, the variation of the refractive index $\eta(\omega)$ across the signal or detection bandwidth is often quite small. In this regime it is a valid approximation to put the square-root factor in the field operator (1.1) equal to its constant value at $\omega=\omega_0$ and to extend the range of integration down to $-\infty$. These narrow-bandwidth approximations are made in all of the calculations that follow. It is also sometimes permissible to ignore the frequency dependence of $\eta(\omega)$ in the exponent in (1.1), and the properties of the electric field in this case are determined by those of the full-range Fourier transformed operators

$$\hat{a}(t) = \left[\frac{1}{2\pi}\right]^{1/2} \int d\omega\, \hat{a}(\omega)\exp(-i\omega t) \ . \tag{1.3}$$

These satisfy the commutation relation

$$[\hat{a}(t),\hat{a}^\dagger(t')]=\delta(t-t') \ . \tag{1.4}$$

The flow of energy, in the narrow-band approximation, is proportional to the flux of the light beam, measured in photons per unit time. This quantity is represented by the flux operator [5]

$$\hat{f}(t) \equiv \hat{a}^\dagger(t)\hat{a}(t)$$
$$= \frac{1}{2\pi}\int d\omega \int d\omega'\, \hat{a}^\dagger(\omega)\hat{a}(\omega')\exp[i(\omega-\omega')t] \ . \tag{1.5}$$

The continuous-mode formalism can handle light beams whose fluxes have arbitrary time dependences, including for example pulse trains and beams of constant mean intensity. The beam in the latter case has a frequency-dependent correlation function of the form

$$\langle \hat{a}^\dagger(\omega)\hat{a}(\omega')\rangle = 2\pi f(\omega)\delta(\omega-\omega') \ , \tag{1.6}$$

where $f(\omega)$ is the beam spectrum, defined as the mean flux per unit ω bandwidth. The total mean flux from (1.5) has the constant value

$$f(t) \equiv \langle \hat{f}(t)\rangle = \int d\omega f(\omega) \equiv F \ , \tag{1.7}$$

in this case.

The calculations that follow assume that the conditions for the validity of the narrow-bandwidth approximations are satisfied, but the time dependences of the light beams are otherwise arbitrary.

II. TRAVELING-WAVE ATTENUATION

A. Beam-splitter model

The scattering centers that cause the attenuation of a light beam in an optical fiber can be modeled [3] by beam splitters of the kind represented in Fig. 1. The output mode operators are given by

$$\hat{a}_{\text{out}}(\omega) = t(\omega)\hat{a}_{\text{in}}(\omega) + r(\omega)\hat{b}(\omega) \ ,$$
$$\hat{a}_s(\omega) = r(\omega)\hat{a}_{\text{in}}(\omega) + t(\omega)\hat{b}(\omega) \ , \tag{2.1}$$

where $r(\omega)$ and $t(\omega)$ are the complex reflection and transmission coefficients of the beam splitter at angular frequency ω. The transformation from input to output operators is unitary if

$$|r(\omega)|^2 + |t(\omega)|^2 = 1 \ ,$$
$$r^*(\omega)t(\omega) + r(\omega)t^*(\omega) = 0 \ , \tag{2.2}$$

and independent boson input operators then produce independent boson output operators. The practical realization of a frequency-dependent beam splitter is outlined in Appendix A.

The time-dependent operators for the beam-splitter input and output modes defined in accordance with (1.3) are not in general simply related on account of the frequency dependence of the reflection and transmission coefficients. However, it is not difficult to show with the use of (2.2) that the integrated input and output fluxes are equal

$$\int dt \{\hat{a}_{\text{out}}^\dagger(t)\hat{a}_{\text{out}}(t) + \hat{a}_s^\dagger(t)\hat{a}_s(t)\}$$
$$= \int dt \{\hat{a}_{\text{in}}^\dagger(t)\hat{a}_{\text{in}}(t) + \hat{b}^\dagger(t)\hat{b}(t)\} \ . \tag{2.3}$$

For the special case of steady-state light beams, where the input operators satisfy (1.6), the mean fluxes are related by

$$\langle \hat{a}_{\text{out}}^\dagger(t)\hat{a}_{\text{out}}(t)\rangle + \langle \hat{a}_s^\dagger(t)\hat{a}_s(t)\rangle$$
$$= \langle \hat{a}_{\text{in}}^\dagger(t)\hat{a}_{\text{in}}(t)\rangle + \langle \hat{b}^\dagger(t)\hat{b}(t)\rangle \ . \tag{2.4}$$

The scattering centers in an optical fiber of length z are modeled [3,16,19] by the line of beam splitters represent-
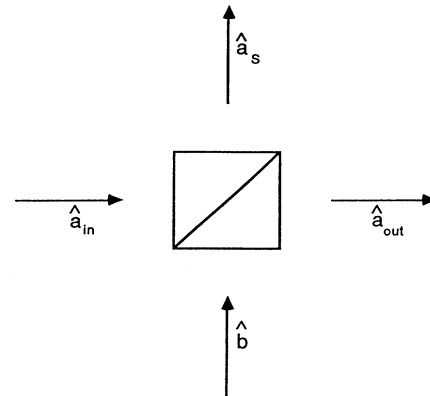

FIG. 1. Attenuating beam splitter.

ed in Fig. 2. These are taken to be discrete components in the initial stages of the calculation, but their number

$$N = z/\Delta z \qquad (2.5)$$

is later taken to infinity in order to model a continuous attenuating medium. The input signal-mode operator $\hat{a}_{\text{in}}(\omega)$ has the commutator

$$[\hat{a}_{\text{in}}(\omega), \hat{a}_{\text{in}}^{\dagger}(\omega')] = \delta(\omega - \omega') , \qquad (2.6)$$

similar to (1.2). The input operators $\hat{b}_n(\omega)$ refer to independent thermally excited modes, and their commutator is

$$[\hat{b}_m(\omega), \hat{b}_n^{\dagger}(\omega')] = \delta_{mn}\delta(\omega - \omega') . \qquad (2.7)$$

A calculation of the effects of attenuation requires an expression for the output signal operator in terms of the input operators. This is readily obtained by iteration of the expression (2.1) for a single beam splitter. Thus taking account of the beam propagation phase with wave vector ω/c, the required expression is

$$\hat{a}_{\text{out}}(\omega) = [t(\omega)e^{i\omega\Delta z/c}]^N \hat{a}_{\text{in}}(\omega)$$

$$+ r(\omega) \sum_{m=1}^{N} [t(\omega)e^{i\omega\Delta z/c}]^{N-m}\hat{b}_m(\omega) . \qquad (2.8)$$

The beam splitters are now converted to a continuous array by taking the limits

$$N \to \infty, \quad \Delta z \to 0, \quad \text{and} \quad |r(\omega)|^2 \to 0 \qquad (2.9)$$

such that the imaginary part of the wave vector

$$\kappa(\omega) = |r(\omega)|^2/2\Delta z \qquad (2.10)$$

remains finite. The usual exponential limit then gives

$$|t(\omega)|^{2N} = [1 - |r(\omega)|^2]^N$$

$$= [1 - 2\kappa(\omega)z/N]^N \to \exp[-2\kappa(\omega)z] . \qquad (2.11)$$

The frequency-dependent phase of the transmission coefficients in (2.8) has the effect of changing the real part of the wave vector from its free-space value ω/c. When the limits (2.9) are taken, this real part, denoted by k, can be expressed in the usual way in terms of a refractive index $\eta(\omega)$,
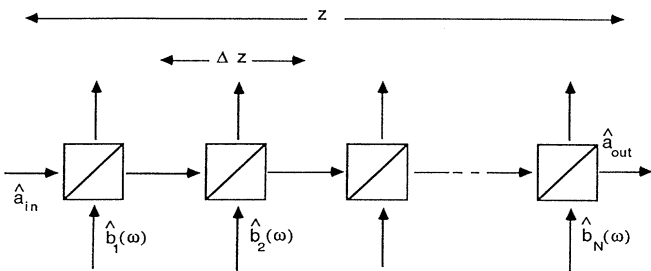
$$k = \omega\eta(\omega)/c . \qquad (2.12)$$

FIG. 2. Beam-splitter representation of scattering in an optical fiber.

The residual phase of the reflection coefficient in the same limit can be chosen to be $\pi/2$.

The thermal input operators and their commutator are converted to continuous spatial dependences by the replacements

$$\hat{b}_m(\omega) \to (\Delta z)^{1/2}\hat{b}(\omega, z') \quad \text{and} \quad \delta_{mn} \to \Delta z\delta(z' - z'') , \qquad (2.13)$$

with the result

$$[\hat{b}(\omega, z'), \hat{b}^{\dagger}(\omega', z'')] = \delta(\omega - \omega')\delta(z' - z'') . \qquad (2.14)$$

These operators are assumed to have the expectation values

$$\langle \hat{b}(\omega, z') \rangle = \langle \hat{b}^{\dagger}(\omega, z') \rangle = 0 \qquad (2.15)$$

and

$$\langle \hat{b}^{\dagger}(\omega, z')\hat{b}(\omega', z'') \rangle = n(T)\delta(\omega - \omega')\delta(z' - z'') , \qquad (2.16)$$

where

$$n(T) = 1/[\exp(\hbar\omega/k_B T) - 1] . \qquad (2.17)$$

The excitation bandwidths are assumed to be sufficiently narrow that the frequency dependence of $n(T)$ can be ignored.

The above developments in conjunction with the usual replacement of summation by integration convert the output operator (2.8) to the form

$$\hat{a}_{\text{out}}(\omega) = \exp[ikz - \kappa(\omega)z]\hat{a}_{\text{in}}(\omega)$$

$$+ i\sqrt{2\kappa(\omega)} \int_0^z dz'\exp\{[ik - \kappa(\omega)](z - z')\}$$

$$\times \hat{b}(\omega, z') . \qquad (2.18)$$

It is not difficult to verify with the use of (2.6) and (2.14) that the output operators have the proper boson commutator,

$$[\hat{a}_{\text{out}}(\omega), \hat{a}_{\text{out}}^{\dagger}(\omega')] = \delta(\omega - \omega') . \qquad (2.19)$$

It is seen from (2.18) that the effect of the attenuation is to reduce the input component of the output operator and to introduce contributions from the noise operators.

The above derivations are concerned only with propagation in the positive z direction. An expression very similar to (2.18) relates the input and output operators for propagation in the negative z direction. In particular, the attenuation produces negative-traveling noise contributions even in the absence of any input signal in this direction.

B. Pulse propagation

The input-output operator relation (2.18) includes the well-known classical effect of optical pulse distortion in a dispersive medium [20]. Consider, for example, an input Gaussian pulse represented by a coherent state [5] with complex amplitude

$$\alpha_{\text{in}}(\omega) = (2\pi\delta^2)^{-1/4}\exp[i(\omega - \omega_0)t_0 - (\omega - \omega_0)^2/4\delta^2] , \qquad (2.20)$$

and

$$\alpha_{\text{in}}(t)=(2\delta^2/\pi)^{1/4}\exp[\,-i\omega_0t_0+\delta^2(t-t_0)^2]\ . \quad (2.21)$$

The pulse properties at the output from the fiber are obtained with the use of (2.18). Suppose for simplicity that the imaginary part of the wave vector $\kappa(\omega)$ has a constant value κ_0 across the pulse bandwidth. A Taylor expansion of the real part of the wave vector around the central frequency of the pulse gives

$$k=k_0+(\omega-\omega_0)k_0'+\tfrac{1}{2}(\omega-\omega_0)^2k_0''+\cdots\ , \quad (2.22)$$

where

$$k_0\equiv\omega_0\eta(\omega_0)/c\ , \quad (2.23)$$

$$k_0'=\frac{\partial k}{\partial\omega}\bigg|_{\omega=\omega_0}=\frac{1}{v_G}\ , \quad (2.24)$$

and k_0'' measures the dispersion in the group velocity v_G. A simple Fourier transform now leads to the mean output amplitude

$$\langle\hat{a}_{\text{out}}(t)\rangle=(2\pi)^{-1/4}(2\Delta^2/\delta)^{1/2}$$
$$\times\exp\{-i\omega_0t+ik_0z-\kappa_0z$$
$$-\Delta^2(t-t_0-k_0'z)^2\}\ , \quad (2.25)$$

where

$$\Delta^2=\delta^2/(1-2i\delta^2k_0''z)\ . \quad (2.26)$$

The pulse therefore travels with the group velocity and its shape remains Gaussian, but with a duration increased by the factor

$$(1+4\delta^4k_0''^2z^2)^{1/2}\ . \quad (2.27)$$

This effect of the group-velocity dispersion in increasing the pulse width is of course well known [20].

C. Direct detection

Suppose that the output from the attenuating fiber is fed into a photodetector of quantum efficiency ζ that runs from time t_0+T_0. The mean photocount is given by

$$\langle m\rangle=\zeta\int_{t_0}^{t_0+T_0}dt\,f_{\text{out}}(t)\ , \quad (2.28)$$

where

$$f_{\text{out}}(t)\equiv\langle\hat{f}_{\text{out}}(t)\rangle \quad (2.29)$$

and

$$\hat{f}_{\text{out}}(t)\equiv\hat{a}_{\text{out}}^{\dagger}(t)\hat{a}_{\text{out}}(t) \quad (2.30)$$

is the operator that represents the output photon flux. The expectation value (2.29) is obtained with the use of (2.18) and the Fourier transform, analogous to (1.5),

$$f_{\text{out}}(t)=\frac{1}{2\pi}\int d\omega\int d\omega'\langle\hat{a}_{\text{in}}^{\dagger}(\omega)\hat{a}_{\text{in}}(\omega')\rangle$$
$$\times\exp\{\,i(\omega-\omega')t-i(k-k')z$$
$$-[\kappa(\omega)+\kappa(\omega')]z\}$$
$$+\frac{n(T)}{2\pi}\int d\omega[1-K(\omega)]\ , \quad (2.31)$$

where k' is the real part of the wave vector at frequency ω' and

$$K(\omega)=\exp[\,-2\kappa(\omega)z] \quad (2.32)$$

is defined to be the attenuation coefficient of the fiber at frequency ω. The first term in (2.31) represents the dispersed and attenuated input flux, while the second term represents a flux of chaotic light, or noise, provided by the scattering of light from thermal sources into the detected beam. This chaotic flux can often be neglected at optical frequencies where $n(T)$ is usually very small.

The output flux can be reexpressed in a simpler form when the input signal has a sufficiently narrow bandwidth that the refractive index and attenuation coefficient can be set equal to their values at the central frequency ω_0 of the signal. Then (2.12) can be approximated by

$$k=\omega\eta(\omega_0)/c\equiv\omega\eta_0/c\ , \quad (2.33)$$

and (2.32) by

$$K_0\equiv K(\omega_0)=\exp[\,-2\kappa(\omega_0)z]\equiv\exp[\,-2\kappa_0z]\ , \quad (2.34)$$

and the output flux (2.31) reduces to

$$f_{\text{out}}(t)=K_0f_{\text{in}}(t_R)+\frac{n(T)}{2\pi}\int d\omega[1-K(\omega)]\ , \quad (2.35)$$

where

$$f_{\text{in}}(t_R)=\langle\hat{a}_{\text{in}}^{\dagger}(t_R)\hat{a}_{\text{in}}(t_R)\rangle \quad (2.36)$$

is the input flux at the retarded time

$$t_R\equiv t-(\eta_0z/c)\ . \quad (2.37)$$

The effects of propagation along the fiber on the input signal in the narrow-band limit clearly correspond to simple physical expectations.

The output flux also simplifies for an input beam of constant mean intensity whose frequency correlation function has the form

$$\langle\hat{a}_{\text{in}}^{\dagger}(\omega)\hat{a}_{\text{in}}(\omega')\rangle=2\pi f_{\text{in}}(\omega)\delta(\omega-\omega')\ , \quad (2.38)$$

in accordance with (1.6). The total mean input flux is thus time independent with the value

$$f_{\text{in}}(t)=\int d\omega\,f_{\text{in}}(\omega)\equiv F_{\text{in}}\ . \quad (2.39)$$

The output correlation function obtained with the use of (2.16), (2.18), and (2.38) is

$$\langle\hat{a}_{\text{out}}^{\dagger}(\omega)\hat{a}_{\text{out}}(\omega')\rangle=2\pi f_{\text{out}}(\omega)\delta(\omega-\omega')\ , \quad (2.40)$$

where

$$f_{\text{out}}(\omega)=K(\omega)f_{\text{in}}(\omega)+[n(T)/2\pi][1-K(\omega)]\ . \quad (2.41)$$

The total mean output flux is

$$f_{\text{out}}(t)=\int d\omega\,f_{\text{out}}(\omega)\equiv F_{\text{out}}\ . \quad (2.42)$$

The output spectrum depends of course on the frequency dependences of the input flux and the attenuation coefficient. We consider again a narrow-band input, for example, the "single-mode" coherent state $|\{\alpha_{\text{in}}\}\rangle$ with [5]

$$\alpha_{in}(\omega) = (2\pi F_{in})^{1/2} \exp(i\phi_{in}) \delta(\omega - \omega_0) ,$$

$$\tag{2.43}$$

$$\alpha_{in}(t) = F_{in}^{1/2} \exp(-i\omega_0 t + i\phi_{in}) ,$$

where the total output flux is

$$F_{out} = K_0 F_{in} + [n(T)/2\pi] \int d\omega [1 - K(\omega)] . \tag{2.44}$$

The mean photocount is obtained from (2.28) and (2.29) with the use of (2.35) or (2.44) as appropriate.

The variance in the direct-detection photocount for an input beam of constant mean intensity is given by [5]

$$(\Delta m)^2 = \langle m \rangle + \zeta^2 \int_{t_0}^{t_0+T_0} dt \int_{t_0}^{t_0+T_0} dt' \{ \langle :\hat{f}_{out}(t)\hat{f}_{out}(t'): \rangle - F_{out}^2 \} , \tag{2.45}$$

where the colons denote normal ordering. This can again be expressed in terms of the input and thermal operators with the use of (2.18). The factorization property

$$\langle \hat{b}^\dagger(\omega,z')\hat{b}^\dagger(\omega',z'')\hat{b}(\omega'',z''')\hat{b}(\omega''',z'''') \rangle = \langle \hat{b}^\dagger(\omega,z')\hat{b}(\omega'',z''') \rangle \langle \hat{b}^\dagger(\omega',z'')\hat{b}(\omega''',z'''') \rangle$$

$$+ \langle \hat{b}^\dagger(\omega,z')\hat{b}(\omega''',z'''') \rangle \langle \hat{b}^\dagger(\omega',z'')\hat{b}(\omega'',z''') \rangle \tag{2.46}$$

enables the chaotic noise contribution to be evaluated in terms of the expectation value (2.16). The general result is quite complicated, and we present only the special case of the coherent input specified by (2.43) when the integrand in (2.45) takes the form

$$\langle :\hat{f}_{out}(t)\hat{f}_{out}(t'): \rangle - F_{out}^2 = K_0 F_{in} [n(T)/\pi] \int d\omega [1 - K(\omega)] \cos[(\omega_0 - \omega)\tau]$$

$$+ [n(T)/2\pi]^2 \left| \int d\omega [1 - K(\omega)] \exp(-i\omega\tau) \right|^2 , \tag{2.47}$$

where

$$\tau = t - t' . \tag{2.48}$$

The above expression clearly vanishes for zero attenuator temperature T, when (2.45) reduces to

$$(\Delta m)^2 = \langle m \rangle , \tag{2.49}$$

the usual shot-noise result expected for the photodetection of purely coherent light.

D. Balanced homodyne detection

The measurement made by a balanced homodyne detector that runs from time t_0 to time $t_0 + T_0$ is represented by the operator [5,21]

$$\hat{O} = i \int_{t_0}^{t_0+T_0} dt \{ \hat{a}^\dagger(t)\hat{a}_L(t) - \hat{a}_L^\dagger(t)\hat{a}(t) \} \tag{2.50}$$

corresponding to the difference between the integrated photocounts in the two detector arms. Here $\hat{a}(t)$ can be the fiber input or output operator, and $\hat{a}_L(t)$ is the local oscillator operator. The local oscillator is assumed to be in a coherent state $|\{\alpha_L\}\rangle$ with a very narrow spread of frequencies, so that its amplitude has the single-mode form

$$\alpha_L(t) = F_L^{1/2} \exp(i\phi_L - i\omega_0 t) , \tag{2.51}$$

where F_L is the mean flux of the local oscillator light in units of photons per unit time, and ϕ_L is its phase angle. Then if the local oscillator is much more intense than the signal, it is a good approximation to replace the local oscillator operators in (2.50) by the corresponding c-numbers, and the measurement operator can be written

$$\hat{O} = (F_L T_0)^{1/2} \hat{E}(\phi_L, t_0) \tag{2.52}$$

where

$$\hat{E}(\phi_L, t_0) = T_0^{-1/2} \int_{t_0}^{t_0+T_0} dt [i\hat{a}^\dagger(t)\exp(-i\omega_0 t + i\phi_L)$$

$$- i\hat{a}(t)\exp(i\omega_0 t - i\phi_L)] . \tag{2.53}$$

The dimensionless electric-field operator defined in this way represents the property of the signal field that is measured in balanced homodyne detection.

The mean difference photocount in balanced homodyne detection of the output from the attenuating fiber is

$$\langle m \rangle = \zeta \langle \hat{O} \rangle = \zeta (F_L T_0)^{1/2} \langle \hat{E}_{out}(\phi_L, t_0) \rangle , \tag{2.54}$$

where ζ is again the detector quantum efficiency. The output-field expectation value is related to the input-field expectation value by means of (1.3) and (2.18). We assume that the input signal has a narrow bandwidth centered on the same frequency as the local oscillator so that any deviations of the refractive index and attenuation coefficient from their values η_0 and K_0 at frequency ω_0 are insignificant. The output-field expectation value is then given by

$$\langle \hat{E}_{out}(\phi_L, t_0) \rangle = (K_0)^{1/2} \langle \hat{E}_{in}(\phi_{LR}, t_{0R}) \rangle , \tag{2.55}$$

where the retarded local oscillator phase and detection period, defined by

$$\phi_{LR} = \phi_L - \frac{\omega_0 \eta_0 z}{c}, \quad t_{0R} = t_0 - \frac{\eta_0 z}{c} , \tag{2.56}$$

merely compensate the time taken for the signal to travel through the fiber.

The balanced homodyne detection photocount variance is given by [5]

$$(\Delta m)^2 = \zeta(1-\zeta)F_L T_0 + \zeta^2 F_L T_0 \langle [\Delta \hat{E}_{out}(\phi_L, t_0)]^2 \rangle . \tag{2.57}$$

The output-field variance is related to the input-field variance by means of (1.3) and (2.18), and making use of the noise operator properties (2.14) and (2.16), we find

$$\langle [\Delta \hat{E}_{\text{out}}(\phi_L, t_0)]^2 \rangle = K_0 \langle [\Delta \hat{E}_{\text{in}}(\phi_{LR}, t_{0R})]^2 \rangle + 2[2n(T)+1] \int d\omega [1 - K(\omega)] \sin^2[(\omega_0 - \omega)T_0/2]/\pi(\omega_0 - \omega)^2 T_0 \; . \quad (2.58)$$

The magnitude of the added noise term depends on the profile $K(\omega)$ of the attenuation, but a simple result emerges when the integration time is sufficiently long and the dispersion in the attenuation coefficient is sufficiently small that the inequality

$$T_0 \gg \frac{1}{K_0} \frac{dK(\omega)}{d\omega} \bigg|_{\omega = \omega_0} \quad (2.59)$$

is satisfied. The final factors in the integrand of (2.58) then have the effect of a delta function, and the result reduces to

$$(\Delta E_{\text{out}})^2 = K_0 (\Delta E_{\text{in}})^2 + [2n(T)+1](1 - K_0) \; , \quad (2.60)$$

where the field variances are written in abbreviated notation. The added noise represented by the second term on the right takes its minimum value for zero temperature, when the result can be written [19]

$$(\Delta E_{\text{out}})^2 - 1 = K_0 [(\Delta E_{\text{in}})^2 - 1] \; . \quad (2.61)$$

It follows that the noise tends to the value 1, characteristic of coherent light, under conditions of severe attenuation when $K_0 \ll 1$. It is easily shown from (2.58) that this conclusion holds generally provided that $K(\omega)$ is very small throughout the detection bandwidth.

The effects of attenuation on the homodyne electric-field operator of (2.53) can be written in compact forms in terms of the operator

$$\hat{F} = \hat{E}_{\text{out}}(\phi_L, t_0) - (K_0)^{1/2} \hat{E}_{\text{in}}(\phi_{LR}, t_{0R}) \; , \quad (2.62)$$

when (2.55) and (2.60) take the forms

$$\langle \hat{F} \rangle = 0 \; , \quad (2.63)$$

and

$$(\Delta F)^2 = [2n(T)+1](1 - K_0) \; . \quad (2.64)$$

This last result has exactly the form of the standard fluctuation-dissipation theorem [22], where the factor $1 - K_0$ represents the dissipation in the attenuator.

The above calculations refer to homodyne measurements made at a given distance z along an attenuating optical fiber. We now consider the compatibility between measurements made at different distances z and z' with different local oscillator phase angles ϕ_L and ϕ_L', and with integration periods T_0 that commence at different times t_0 and t_0'. The required homodyne field commutation relation, obtained with the use of (1.3) and (2.18), is

$$[\hat{E}_{\text{out}}(\phi_L, t_0, z), \hat{E}_{\text{out}}(\phi_L', t_0', z')] = -\frac{4i}{\pi T_0} \int d\omega \exp[-\kappa(\omega)|z - z'|] \sin[\phi_L - \phi_L' - k(z - z') + (\omega - \omega_0)(t_0 - t_0')]$$

$$\times \sin^2[(\omega - \omega_0)T_0/2]/(\omega - \omega_0)^2 \; , \quad (2.65)$$

where the field operators are given by (2.53) with their notation expanded to show the propagation distance.

The commutator can be set into a more explicit form only if $\kappa(\omega)$ and $\eta(\omega)$ are assigned specific functional forms. We consider here only the simplest case in which these functions have constant values κ_0 and η_0, corresponding to negligible dispersion over a frequency range of order $1/T_0$ around ω_0. The wave vector can then be approximated by (2.33), and the sine that contains it can be expanded in terms that contain the contribution proportional to $(\omega - \omega_0)$ and the frequency-independent remainder. The integration in (2.65) can then be performed using standard results [23], and the commutator becomes

$$[\hat{E}_{\text{out}}(\phi_L, t_0, z), \hat{E}_{\text{out}}(\phi_L', t_0', z')] = -\frac{2i}{T_0} \exp[-\kappa_0 |z - z'|] \sin[\phi_L - \phi_L' - \omega_0 \eta_0 (z - z')/c]$$

$$\times [T_0 - |t_0 - t_0' - \eta_0 (z - z')/c|] \Theta(T_0 - |t_0 - t_0' - \eta_0 (z - z')/c|) \; , \quad (2.66)$$

where Θ is the usual unit step function. The uncertainty relation that follows from (2.66) is

$$\langle [\Delta \hat{E}_{\text{out}}(\phi_L, t_0, z)]^2 \rangle \langle [\Delta \hat{E}_{\text{out}}(\phi_L', t_0', z')]^2 \rangle \geq \exp[-2\kappa_0 |z - z'|] \sin^2[\phi_L - \phi_L' - \omega_0 \eta_0 (z - z')/c] \mathcal{O} \; , \quad (2.67)$$

where the overlap $\mathcal{O}$ is

$$\mathcal{O} \equiv [1 - |t_0 - t_0' - \eta_0 (z - z')/c|/T_0]^2 \Theta[T_0 - |t_0 - t_0' - \eta_0 (z - z')/c|] \; . \quad (2.68)$$

This function determines the fractional overlap between the sections of the propagating signal that are sampled by the detection windows at coordinates z and z'. In the absence of any overlap, the uncertainty relation (2.67) provides no restriction on the field variances at the two positions. The maximum value of the uncertainty product occurs for complete overlap, where

$$t_0' = t_0 + \eta_0 (z' - z)/c \; , \quad (2.69)$$

and both detection processes observe exactly the same section of the signal beam; the function defined in (2.68) is equal

to unity in this case.

An example that realizes the minimum uncertainty product is provided by a squeezed vacuum state input in the limit of an integration time T_0 that is much longer than the correlation times of the light. The input-field variance is then [21,24]

$$\langle [\Delta E_{\text{in}}(\phi_L, t_0)]^2 \rangle = \exp(2s)\cos^2\left[\phi_L - \frac{\theta}{2}\right] + \exp(-2s)\sin^2\left[\phi_L - \frac{\theta}{2}\right] , \qquad (2.70)$$

where s and θ are the usual parameters that describe the amplitude and phase of the squeezing. Minimum variance product is achieved by making one of the measurements at $z = 0$, so that one of the output fields in the uncertainty relation (2.67) becomes the same as the input field. Then choosing

$$\theta = 2\phi_L - \pi \qquad (2.71)$$

it follows that

$$\langle [\Delta E_{\text{out}}(\phi_L, t_0, 0)]^2 \rangle = \langle [\Delta E_{\text{in}}(\phi_L, t_0)]^2 \rangle = \exp(-2s) . \qquad (2.72)$$

The field variance obtained from (2.60) and (2.70) at an arbitrary position z' is

$$\langle [\Delta \hat{E}_{\text{out}}(\phi'_L, t'_0, z')]^2 \rangle = \exp(-2\kappa_0 z')[\exp(2s)\sin^2(\phi'_L - \phi_L - \omega_0 \eta_0 z'/c)$$
$$+ \exp(-2s)\cos^2(\phi'_L - \phi_L - \omega_0 \eta_0 z'/c)] + 1 - \exp(-2\kappa_0 z') , \qquad (2.73)$$

where the temperature T has been set equal to zero in the interests of reducing the noise as much as possible. If the squeezing amplitude s is now allowed to become infinite, the product of the variances (2.72) and (2.73) is

$$\langle [\Delta \hat{E}_{\text{out}}(\phi_L, t_0, 0)]^2 \rangle \langle [\Delta \hat{E}_{\text{out}}(\phi'_L, t'_0, z')]^2 \rangle$$
$$= \exp(-2\kappa_0 z')\sin^2(\phi'_L - \phi_L - \omega_0 \eta_0 z'/c) , \qquad (2.74)$$

in agreement with the minimum value permitted by the uncertainty relation (2.67), the overlap function being essentially equal to unity for the steady-state light beam considered in this example.

More generally, the presence of the overlap function in (2.67) reflects the well-known requirement that measurements at two space-time points can interfere only if one measurement can communicate with the other, that is, if the two points lie on the same light line [25]. A further impediment to communication between the two measurement points is provided by attenuation, and the associated decaying exponential in the uncertainty relation (2.67) further restricts the interference to points whose spatial separation is of the order of the characteristic attenuation distance or less.

III. TRAVELING-WAVE AMPLIFICATION

A. Beam-splitter model

Optical signals can be continuously amplified as they propagate along a fiber, for example, by stimulated Raman scattering or by interaction with an inverted atomic population. The process can be modeled by a line of beam splitters similar to that shown in Fig. 1 but with modified input-output relations. The amplifying property of the beam splitter is achieved by inverting the harmonic oscillator associated with the thermally excited $\hat{b}(\omega)$ input mode and assigning a negative temperature to the thermal excitation. The harmonic oscillator associated with the scattered $\hat{a}_s(\omega)$ output mode must also be invert-

ed for consistency of the model.

With these modifications, the beam-splitter output and input mode operators are related by

$$\hat{a}_{\text{out}}(\omega) = t(\omega)\hat{a}_{\text{in}}(\omega) + r(\omega)\hat{b}^\dagger(\omega) ,$$
$$\hat{a}_s(\omega) = r(\omega)\hat{a}_{\text{in}}^\dagger(\omega) + t(\omega)\hat{b}(\omega) , \qquad (3.1)$$

where the complex coupling coefficients now satisfy

$$|t(\omega)|^2 - |r(\omega)|^2 = 1 \qquad (3.2)$$

in contrast to the conventional beam-splitter properties in (2.2). The relation (3.2) ensures that the independent input mode operators produce independent output mode operators. The time-dependent mode operators are defined by (1.3) as before and it is not difficult to show that the integrated input and output fluxes satisfy

$$\int dt \{\hat{a}_{\text{out}}^\dagger(t)\hat{a}_{\text{out}}(t) - \hat{a}_s^\dagger(t)\hat{a}_s(t)\}$$
$$= \int dt \{\hat{a}_{\text{in}}^\dagger(t)\hat{a}_{\text{in}}(t) - \hat{b}^\dagger(t)\hat{b}(t)\} . \qquad (3.3)$$

This expression represents energy conservation at the beam splitter, with the negative contributions corresponding to inverted oscillators [26]. In the special case of steady-state light beams, the mean fluxes are related by

$$\langle \hat{a}_{\text{out}}^\dagger(t)\hat{a}_{\text{out}}(t) \rangle - \langle \hat{a}_s^\dagger(t)\hat{a}_s(t) \rangle$$
$$= \langle \hat{a}_{\text{in}}^\dagger(t)\hat{a}_{\text{in}}(t) \rangle - \langle \hat{b}^\dagger(t)\hat{b}(t) \rangle . \qquad (3.4)$$

The line of beam splitters shown in Fig. 2, now assumed to have the amplifying properties described above, is converted to a continuous array by steps similar to those used for the attenuating fiber in (2.9), (2.11), and (2.13). The imaginary part of the wave vector is defined by

$$g(\omega) = |r(\omega)|^2/2\Delta z , \qquad (3.5)$$

similar to (2.10), but with the use of (3.2)

$$|t(\omega)|^{2N} = [1 + |r(\omega)|^2]^N$$
$$= [1 + 2g(\omega)z/N]^N \rightarrow \exp[2g(\omega)z] , \quad (3.6)$$

which represents optical gain, in contrast to the attenuation expressed by (2.11). The output operator obtained by iteration of (3.1) is thus [13,17]

$$\hat{a}_{\text{out}}(\omega) = \exp[ikz + g(\omega)z]\hat{a}_{\text{in}}(\omega)$$
$$+ i\sqrt{2g(\omega)} \int_0^z dz' \exp\{[ik + g(\omega)](z - z')\}$$
$$\times \hat{b}^\dagger(\omega, z') . \quad (3.7)$$

The real part k of the wave vector is still given by (2.12), where the refractive index $\eta(\omega)$ now includes the effects of the gain process. The thermal mode correlation function is given by (2.16) but with the mean photon number of (2.17) evaluated at $|T|$, since the temperature T itself is now negative.

The relation (3.7) between input and output operators has a form that agrees precisely with the relation derived by Caves [27] in his general theory of linear amplifiers. In accordance with this theory, the square modulus of the prefactor of $\hat{a}_{\text{in}}(\omega)$ is taken to be the gain coefficient, given by

$$G(\omega) = \exp[2g(\omega)z] , \quad (3.8)$$

while the second term on the right-hand side represents the noise added by the amplifier. The forms of these terms are such that the output commutator retains its value given by (2.19).

B. Direct detection

The basic calculation of the mean photocount in direct detection described by (2.28) to (2.31) can be applied to the output from an amplifying fiber by substitution of the output operator from (3.7) to (2.31). The results are similar in outline to those for an attenuating fiber, but there are important differences in detail. Thus for an input beam of constant mean intensity, where (2.28) to (2.40) are valid, the output spectrum analogous to (2.41) is

$$f_{\text{out}}(\omega) = G(\omega)f_{\text{in}}(\omega) + [(n(|T|) + 1)/2\pi][G(\omega) - 1] . \quad (3.9)$$

The two terms on the right-hand side represent, respectively, the amplified input flux and the noise added by the amplification process. Some additional noise is inevitable since the latter term does not vanish even for zero negative temperature, when it takes a limiting minimum value in accordance with the requirements of the general theory of linear amplifiers [27].

The expression (3.9) for the amplified flux can be obtained from the expression (2.41) for the attenuated flux by means of the formal replacements

$$K(\omega) \rightarrow G(\omega) \quad \text{and} \quad T \rightarrow -T , \quad (3.10)$$

if use is made of the property

$$n(T) = n(-|T|) = -n(|T|) - 1 \quad (3.11)$$

of the thermal function (2.17) for negative temperatures. The thermal factor in (3.9) applies directly to Raman or nondegenerate parametric amplification where $n(|T|)$ denotes the population of the material excitation or idler photon, respectively, that contributes to the amplification process. For amplification by an inverted atomic population with N_u and N_l atoms in the upper and lower levels, respectively, the population factor that occurs in standard theory [28,29] is

$$P(T) = \frac{N_u}{N_u - N_l} = n(|T|) + 1 , \quad (3.12)$$

where the ratio of populations is described by a Boltzmann factor with negative temperature,

$$N_u/N_l = \exp(\hbar\omega/k_B|T|) . \quad (3.13)$$

Thus perfect inversion with $N_l = 0$ corresponds to $|T| = 0$ with minimum noise flux in (3.9), while imperfect inversion produces a nonzero $n(|T|)$ with an enhanced noise flux.

The mean photocount is readily obtained from (2.28) for the single-mode coherent input described by (2.43), when the mean output flux obtained from (2.42), with the gain coefficient (3.8) at $\omega = \omega_0$ denoted by G_0, is

$$F_{\text{out}} = G_0 F_{\text{in}} + \{[n(|T|) + 1]/2\pi\} \int d\omega[G(\omega) - 1] . \quad (3.14)$$

The detailed form of the frequency integral depends upon the gain function $g(\omega)$. The integral can be evaluated in some important special cases, the simplest being that of a constant gain profile of angular frequency bandwidth B centered on the input frequency ω_0,

$$g(\omega) = g_0 \Theta(\omega - \omega_0 + B/2)\Theta(-\omega + \omega_0 + B/2) , \quad (3.15)$$

when (3.14) reduces to

$$F_{\text{out}} = G_0 F_{\text{in}} + \frac{n(|T|) + 1}{2\pi} B(G_0 - 1) . \quad (3.16)$$

The analogous results for Lorentzian and Gaussian gain profiles are given in Appendix B.

The variance in the direct detection photocount is obtained from (2.45), with the output photon fluxes given by (2.30) and the output photon operators given by the Fourier transform of (3.7). Because of the occurrence of $\hat{b}^\dagger$ in this last expression, normal ordering of the output operators produces antinormal ordering of the thermal operators. However, the required expectation values are straightforwardly calculated by factorizations similar to (2.46) and use of the basic properties (2.14) and (2.16) of the thermal operators. The general result is again complicated and we consider only the special case of a coherent input specified by (2.43), when the integrand in (2.45) simplifies to

$$\langle :\hat{f}_{\text{out}}(t)\hat{f}_{\text{out}}(t'): \rangle - F_{\text{out}}^2 = G_0 F_{\text{in}} \{ [n(|T|)+1]/\pi \} \int d\omega [G(\omega)-1]\cos[(\omega_0 - \omega)\tau]$$

$$+ \{ [n(|T|)+1]/2\pi \}^2 \left| \int d\omega [G(\omega)-1]\exp(-i\omega\tau) \right|^2 . \tag{3.17}$$

These terms survive even for a perfectly inverted amplifier with $|T|=0$, and they represent, respectively, the beating of the amplified coherent input with the noise flux given by the second term in (3.14) and the beating of this chaotic noise with itself. The integrals in (3.17) are readily evaluated for the constant gain profile (3.15), with the result

$$\langle :\hat{f}_{\text{out}}(t)\hat{f}_{\text{out}}(t'): \rangle - F_{\text{out}}^2 = G_0(G_0-1)F_{\text{in}}\frac{n(|T|)+1}{\pi}\frac{2}{\tau}\sin\left[\frac{B\tau}{2}\right] + (G_0-1)^2\left[\frac{n(|T|)+1}{2\pi}\right]^2\left[\frac{2}{\tau}\right]^2\sin^2\left[\frac{B\tau}{2}\right] .$$

$$\tag{3.18}$$

The intensity fluctuation spectrum that can be measured by direct detection is determined from the Fourier transform of (3.17) according to

$$S(\omega) = \zeta F_{\text{out}} + \zeta^2 \int_{-\infty}^{\infty} d\tau \{ \langle :\hat{f}_{\text{out}}(0)\hat{f}_{\text{out}}(\tau): \rangle - F_{\text{out}}^2 \}\exp(i\omega\tau) . \tag{3.19}$$

The τ integral is readily evaluated to give

$$S(\omega) = \zeta G_0 F_{\text{in}} + \zeta \{ [n(|T|)+1]/2\pi \} \int d\omega'[G(\omega')-1] + \zeta^2 G_0 F_{\text{in}}[n(|T|)+1][G(\omega_0-\omega)+G(\omega_0+\omega)-2]$$

$$+ \zeta^2 \{ [n(|T|)+1]^2/2\pi \} \int d\omega'[G(\omega')-1][G(\omega'-\omega)-1] . \tag{3.20}$$

The four contributions to the noise spectrum are similar to those found in conventional amplifier theory. Thus the first two terms, which are independent of the frequency, represent the shot noise in the detection of the amplified signal and spontaneously emitted light, respectively. The frequency dependence of the spectrum arises from the third and fourth terms, which as in (3.17) represent, respectively, the excess noise produced by the beating of the amplified signal with the amplified spontaneous emission, and the beating of the amplified spontaneous emission with itself. These contributions are illustrated by the example of the constant gain profile (3.15), where

$$S(\omega) = \zeta G_0 F_{\text{in}} + \zeta(G_0-1)\frac{n(|T|)+1}{2\pi}B + 2\zeta^2 G_0(G_0-1)F_{\text{in}}[n(|T|)+1]\Theta(B/2-\omega)$$

$$+ \zeta^2(G_0-1)^2\{ [n(|T|)+1]^2/2\pi \}(B-\omega)\Theta(B-\omega) . \tag{3.21}$$

Analogous results for the Lorentzian and Gaussian gain profiles are given in Appendix B.

In experiments with a sufficiently strong coherent input flux F_{in} it is possible to achieve conditions where the noise spectrum is dominated by the first and third terms on the right-hand side of (3.20) or (3.21). Measurements of the noise as a function of the traveling-wave gain in this case can provide values for the thermal excitation factor $n(|T|)$, a quantity that is difficult to determine for some inverted-population amplifiers [30].

C. Balanced homodyne detection

The effects of amplification on the measured mean and variance in balanced homodyne detection are determined by calculations that are very similar to those given in Sec. II D for the effects of attenuation. The relation between the homodyne field operators before and after amplification is now obtained from (2.53) by substitution of the input-output relation (3.7). The mean and the variance of the difference photocount are still given by (2.54) and (2.57), but (2.55) and (2.58) are replaced by

$$\langle \hat{E}_{\text{out}}(\phi_L, t_0) \rangle = (G_0)^{1/2} \langle \hat{E}_{\text{in}}(\phi_{LR}, t_{0R}) \rangle , \tag{3.22}$$

where G_0 is again the gain coefficient at frequency ω_0, and

$$\langle [\Delta\hat{E}_{\text{out}}(\phi_L, t_0)]^2 \rangle = G_0\langle [\Delta\hat{E}_{\text{in}}(\phi_{LR}, t_{0R})]^2 \rangle + 2[2n(|T|)+1]\int d\omega[G(\omega)-1]\sin^2[(\omega_0-\omega)T_0/2]/[\pi(\omega_0-\omega)^2 T_0] .$$

$$\tag{3.23}$$

In the limit of a long integration time, analogous to (2.59), the variance reduces to

$$(\Delta E_{\text{out}})^2 = G_0(\Delta E_{\text{in}})^2 + [2n(|T|)+1](G_0-1) . \tag{3.24}$$

The added noise represented by the second term on the right-hand side is again minimized for zero temperature, when the result can be written

$$(\Delta E_{\text{out}})^2 + 1 = G_0[(\Delta E_{\text{in}})^2 + 1] . \tag{3.25}$$

Thus, in contrast to the corresponding result (2.61) for attenuation, the noise is always increased by amplification.

The mean and the variance of the homodyne electric-field operator can again be written in compact forms in terms of an operator $\hat{F}$ similar to that defined in (2.62) but

with the attenuation coefficient replaced by the gain coefficient. The fluctuation-dissipation theorem analogous to (2.64) is

$$(\Delta F)^2 = [2n(|T|)+1](G_0-1) . \tag{3.26}$$

The output signal from the amplifier shows squeezing if

$$(\Delta E_{\text{out}})^2 < 1 , \tag{3.27}$$

and it follows from (3.24) that this condition is satisfied if

$$G_0 < \frac{2n(|T|)+2}{(\Delta E_{\text{in}})^2+2n(|T|)+1} . \tag{3.28}$$

The gain is thus restricted to very modest values, even for a perfectly squeezed input, with $s \to \infty$ and $\theta = 2\phi_L - \pi$ in the variance (2.70), and an amplifier with complete population inversion, where (3.28) reduces to

$$G_0 < 2 \quad \text{for } (\Delta E_{\text{in}})^2 = 0 \text{ and } n(|T|) = 0 . \tag{3.29}$$

The maximum twofold gain for the preservation of

squeezing is a well-known property of the single-mode cavity amplifier [28,31,32] and the above analysis shows that the same limitation applies to the traveling-wave amplifier.

The compatibility between measurements made at different distances along an amplifying optical fiber with different local oscillator phases and different times of commencement for the integration period is treated by the same methods as used for the attenuating fiber in Sec. II D. Thus the homodyne field commutation relation is the same as (2.65) but with the wave vector $\kappa(\omega)$ replaced by $-g(\omega)$. The commutator (2.66) and the uncertainty relation (2.67) in the limit of negligible dispersion are converted to the case of an amplifying fiber by the replacement of $-\kappa_0$ by $g_0 \equiv g(\omega_0)$. The remarks that follow (2.68) apply with equal force to the amplifying fiber. The minimum uncertainty product is again realized by a squeezed vacuum state input, with variance given by (2.70). Thus one of the measured variances is given by (2.72) while the other is given by (3.24) in the form

$$\langle [\Delta E_{\text{out}}(\phi'_L,t'_0,z')]^2 \rangle = \exp(2g_0z')[\exp(2s)\sin^2(\phi'_L-\phi_L-\omega_0\eta_0z'/c)$$
$$+\exp(-2s)\cos^2(\phi'_L-\phi_L-\omega_0\eta_0z'/c)]+\exp(2g_0z')-1 . \tag{3.30}$$

The product of (2.72) with (3.30) in the limit of an infinitely squeezed input state gives the same result as (2.74) but with $-\kappa_0$ replaced by g_0. The product thus has the minimum value permitted by the uncertainty relation.

It is seen that the minimum uncertainty product for both attenuating and amplifying fibers has common factors of the trigonometric function of local oscillator phase given in (2.67) and the overlap function given by (2.68). The remaining exponential factor in each case is identical to the factor by which the signal intensity is changed by propagation from one observation point to the other. The significance of this factor in terms of communication between two measurement points in an attenuating fiber is discussed at the end of Sec. II D. In the case of an amplifying fiber, the interference between measurements at points that lie on the same light line is increased by the amplification, with a resulting exponential growth in minimum uncertainty product as the spatial separation of the two points is increased.

The results of Sec. II D are readily combined with those of the present section for an optical fiber that simultaneously has an attenuation wave vector $\kappa(\omega)$ and a gain wave vector $g(\omega)$. The generalization of (2.18) and (3.7) is

$$\hat{a}_{\text{out}}(\omega) = \exp\{[ik+g(\omega)-\kappa(\omega)]z\}\hat{a}_{\text{in}}(\omega)$$
$$+i\int_0^z dz'\exp\{[ik+g(\omega)-\kappa(\omega)](z-z')\}$$
$$\times[\sqrt{2g(\omega)}\hat{b}^\dagger_+(\omega,z')+\sqrt{2\kappa(\omega)}\hat{b}_-(\omega,z')], \tag{3.31}$$

where the $+$ $(-)$ subscripts denote the independent thermal input modes associated with the amplification (attenuation). The relation between the input and output

homodyne field operators is readily calculated as before. Thus for a narrow-band input signal, the mean-field results (2.55) and (3.22) are generalized to

$$\langle \hat{E}_{\text{out}}(\phi_L,t_0) \rangle = (G_0K_0)^{1/2}\langle \hat{E}_{\text{in}}(\phi_{LR},t_{0R}) \rangle , \tag{3.32}$$

while the variance results (2.60) and (3.24) in the limit of a long integration time are generalized to

$$(\Delta E_{\text{out}})^2 = G_0K_0(\Delta E_{\text{in}})^2$$
$$+\frac{G_0K_0-1}{g_0-\kappa_0}\{g_0[2n_+(|T|)+1]$$
$$+\kappa_0[2n_-(T)+1]\} . \tag{3.33}$$

There is particular practical interest in the achievement of optical transmission lines in which the fiber loss is exactly compensated by gain, so that $g_0 = \kappa_0$, and the input and output means and variances are related by

$$\langle \hat{E}_{\text{out}}(\phi_L,t_0) \rangle = \langle \hat{E}_{\text{in}}(\phi_{LR},t_{0R}) \rangle \tag{3.34}$$

and

$$(\Delta E_{\text{out}})^2 = (\Delta E_{\text{in}})^2+4\kappa_0z \quad (g_0=\kappa_0) , \tag{3.35}$$

where the thermal mode temperatures have been set equal to zero. The added noise thus grows linearly with the propagation distance. For gain-compensated low-loss optical fiber with

$$\kappa_0 = 0.023 \text{ km}^{-1} \quad (=0.2 \text{ dB/km}) , \tag{3.36}$$

and for a highly squeezed input with essentially zero noise, the squeezing defined by the inequality (3.27) is lost after a propagation distance of about 11 km.

IV. CONCLUSIONS

We have applied the one-dimensional continuous-mode quantization method of Blow *et al.* [5] to the problems of electromagnetic wave propagation in attenuating and amplifying optical fibers. With the use of simple beam-splitter models of the scattering centers and the amplification processes in the fiber, the formalism embraces both the spatial and temporal variations in the electromagnetic field. The calculations are simplified by the assumption of a narrow-band input signal, in accordance with the usual conditions of optical transmission systems. The field operators satisfy the appropriate quantum-mechanical commutation relations at every point in the fiber, and in particular they conform to the general requirements on the input and output operators of phase-independent amplifiers [27].

In calculations of the effects of attenuation and amplification on the initial statistical properties of the input signal, it is convenient in the continuous-mode formalism to work with measured quantities instead of the abstract operators of the electromagnetic field. We accordingly use simple models of direct and balanced homodyne detection that take account of quantum efficiency and integration time. For direct detection that take account of quantum efficiency and integration time. For direct detection we have calculated the mean and the variance of the integrated photocount, and also the intensity fluctuation spectrum. The results obtained in this case are formally similar to those found for a cavity standing-wave attenuator or amplifier, but the traveling-wave amplifier displays the additional important feature of a gain profile that generally narrows in frequency as the propagation distance is increased.

The mode-matching requirements of homodyne detection with a narrow-band local oscillator have the effect of restricting the measurement to field components of sharply defined propagation direction and frequency. We have calculated the mean and the variance of the homodyne electric field that is selected by such measurements. There are again some similarities between the traveling-wave results and those obtained for lumped or cavity components, and, for example, the restriction to a maximum of twofold amplification for the retention of some squeezing from an infinitely squeezed input signal remains in force. However, there are also specific propagation effects in the traveling-wave attenuator or amplifier, and we have given detailed treatments of the uncertainty relations that govern measurements of the homodyne fields at different space-time points. These are essentially one-dimensional versions of the better-known uncertainty relations that govern the electric fields at different points in three dimensions, and the homodyne field results can be similarly interpreted in terms of the feasibility of communication between the two measurement points.

The noise in both kinds of detection increases with the magnitude of the effective temperature in accordance with the natures of the functions $n(T)$ for attenuation and $n(|T|)$ for amplification. These functions vanish for zero positive or negative temperatures, when the noise

takes its smallest allowed values. This ideal limit can be achieved in practice for Raman amplification, where the scattering material vibration often has negligible thermal excitation [18], but the thermal function is usually much larger than unity for Brillouin amplifiers [29]. In the case of inverted population amplifiers, where the populations of the active levels may be difficult to determine independently, measurements of the amplifier noise provide a useful technique for obtaining this information via the deduced variation of the thermal function with the gain [30].

Finally, it should be emphasized that although many of the results have for the sake of simplicity been illustrated by examples of steady-state coherent inputs, the main input-output operator relations apply to arbitrary input signals, within the overall conditions of validity of the narrow-bandwidth approximations. The results can thus be used to obtain complete information on the temporal and spatial development of traveling-wave signals in attenuating and amplifying fibers.

APPENDIX A: LORENTZIAN BEAM SPLITTER

Figure 3 shows an example of a composite beam splitter that produces a scattered spectrum with a Lorentzian line shape for appropriate values of the parameters. The active element is a Fabry-Pérot étalon that consists of two identical mirrors of infinitesimal thickness separated by a distance d and with complex frequency-independent reflection and transmission coefficients r and t such that
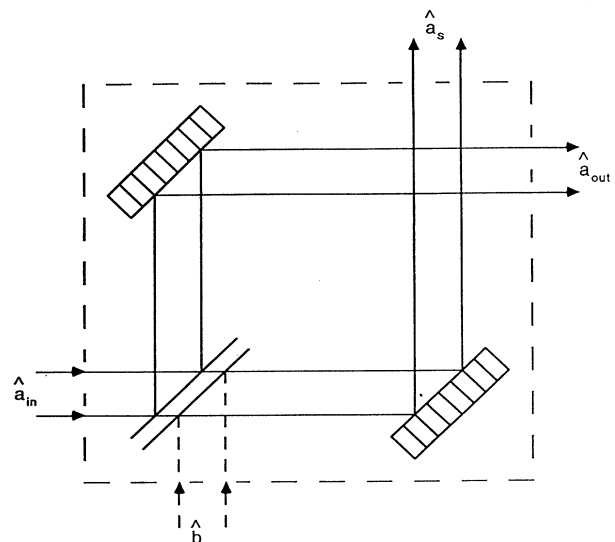

FIG. 3. Model for a Lorentzian beam splitter.

$$|r|^2+|t|^2=1 \quad \text{and} \quad \exp(2i\phi_t)=-\exp(2i\phi_r) \ . \tag{A1}$$

Then with the origin for the optical phase taken in the center of the étalon, it is easily shown that the reflection and transmission coefficients of the composite beam splitter are

$$r(\omega)=-\frac{|t|^2\exp(2i\phi_r)}{1-|r|^2\exp[2i(\phi_r+\phi)]} \ , \tag{A2}$$

and

$$t(\omega)=\frac{\{1-\exp[2i(\phi_r+\phi)]\}|r|\exp(i\phi_r-i\phi)}{1-|r|^2\exp[2i(\phi_r+\phi)]} \ , \tag{A3}$$

where

$$\phi=\omega d/\sqrt{2}c \ . \tag{A4}$$

It is readily verified that these coefficients satisfy the unitarity relations (2.2).

According to (2.10), the attenuation profile of the beam splitter is determined by the function

$$|r(\omega)|^2=|t|^4/[|t|^4+4|r|^2\sin^2(\phi_r+\phi)] \ . \tag{A5}$$

Maximum attenuation occurs at frequencies ω_n given by

$$\omega_n=\sqrt{2}c(n\pi-\phi_r)/d \quad (n=\text{integer}) \ , \tag{A6}$$

and for ω close to ω_n

$$|r(\omega)|^2\simeq\Gamma^2/[(\omega-\omega_n)^2+\Gamma^2] \ , \tag{A7}$$

where

$$\Gamma=|t|^2c/\sqrt{2}|r|d \ . \tag{A8}$$

This Lorentzian scattered spectrum has a full width at half maximum height (FWHM) of 2Γ. The scattering associated with a given mode n of the étalon can be considered in isolation when the adjacent modes are made sufficiently narrow and distant by the choice of appropriately small transmission $|t|$ and mirror separation d. A more versatile composite beam splitter that produces less than 100% scattering at exact resonance can be constructed by the use of different mirrors in the étalon, or more generally by the insertion of additional optical components.

A complete set of modes of the composite frequency-dependent beam splitter is provided by the sets of plane waves of continuous frequency ω that are incident from the directions of the four arms of the beam splitter. It is not difficult to show that the corresponding mode functions have orthonormal properties, provided that the spatial integrations include the propagation paths within the compound beam splitter itself. The modes therefore form a proper basis for the quantization of the optical field in terms of the operators used in (2.1).

APPENDIX B: TRAVELING-WAVE AMPLIFICATION WITH LORENTZIAN OR GAUSSIAN GAIN PROFILES

Consider first the effects of a gain profile that produces a Lorentzian variation of the gain wave vector, with

$$g(\omega)=g_0\gamma^2/[(\omega-\omega_0)^2+\gamma^2] \ . \tag{B1}$$

The full width of the Lorentzian function at half maximum height is

$$W_1=2\gamma \ . \tag{B2}$$

The integral that determines the noise flux in (3.14) is difficult in general, but it can be evaluated simply in two limiting cases.

(i) $g_0z \ll 1$. In this case the gain coefficient (3.8) is approximately

$$G(\omega)=1+\frac{2g_0z\gamma^2}{(\omega-\omega_0)^2+\gamma^2} \ . \tag{B3}$$

We evaluate the various output quantities only for zero noise temperature. The output flux (3.14) is then

$$F_{\text{out}}=G_0F_{\text{in}}+\frac{\gamma}{2}(G_0-1) \ . \tag{B4}$$

The measured intensity fluctuation spectrum (3.20) is similarly evaluated without difficulty to give

$$S(\omega)= \zeta G_0 F_{\text{in}}+\frac{\zeta\gamma}{2}(G_0-1)$$
$$+2\zeta^2G_0(G_0-1)F_{\text{in}}\frac{\gamma^2}{\omega^2+\gamma^2}$$
$$+\zeta^2(G_0-1)^2\frac{\gamma^3}{\omega^2+4\gamma^2} \ . \tag{B5}$$

(ii) $g_0z \gg 1$. In this case of high gain the initial Lorentzian form (B3) of the gain coefficient is distorted to a Gaussian, whose form can be shown to be [33]

$$G(\omega)=G_0\exp[-2g_0z(\omega-\omega_0)^2/\gamma^2] \ . \tag{B6}$$

The width (FWHM) of the gain coefficient is now

$$W_2=[\ln2/\ln(G_0)]^{1/2}2\gamma \ . \tag{B7}$$

The gain profile therefore narrows with increasing values of the peak gain, although it should be noted that very large values of G_0 are needed to achieve a substantial narrowing; for example, the square-root factor in (B7) is equal to 0.25 for $G_0=6.5\times10^4$. The output flux (3.14) is now

$$F_{\text{out}}=G_0F_{\text{in}}+\frac{\gamma}{2}\frac{G_0}{[\pi\ln(G_0)]^{1/2}} \ , \tag{B8}$$

and the intensity fluctuation spectrum (3.20) is

$$S(\omega)= \zeta G_0 F_{\text{in}}+\frac{\zeta\gamma}{2}\frac{G_0}{[\pi\ln(G_0)]^{1/2}}$$
$$+2\zeta^2G_0^2F_{\text{in}}\exp[-\ln(G_0)\omega^2/\gamma^2]$$
$$+\frac{\zeta^2}{2}\frac{G_0^2\gamma}{[2\pi\ln(G_0)]^{1/2}}\exp[-\ln(G_0)\omega^2/2\gamma^2] \ . \tag{B9}$$

Figure 4 shows the variation with peak gain of the noise flux divided by the peak gain. This quantity provides a primitive noise figure for the performance of the
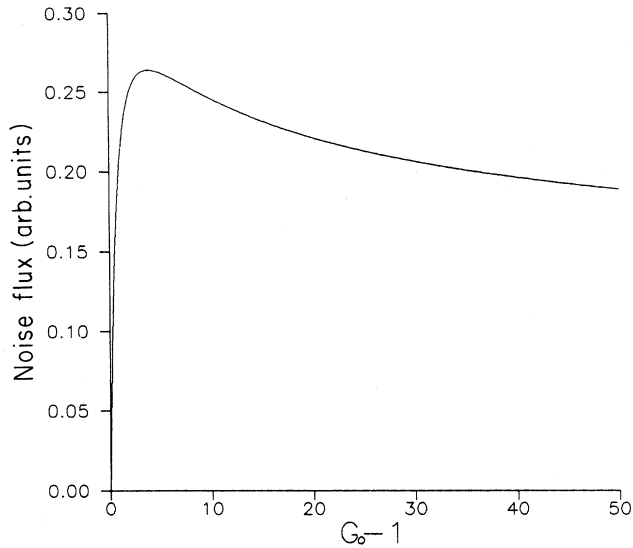
FIG. 4. Variation with peak gain G_0 of the normalized noise flux $\int d\omega[G(\omega)-1]/2\pi\gamma G_0$ obtained from (3.14) for zero amplifier temperature.

traveling-wave amplifier. The steeply increasing part of the curve for small G_0 corresponds to the Lorentzian profile, while the Gaussian profile becomes a good approximation for gains much larger than those included in the figure. The form of the output flux given in (B8) shows that the slow falloff in noise figure continues to these larger values of the peak gain, and, for example, it takes the value 0.125 for $G_0 = 1000$.

Now consider a Gaussian variation of the wave vector given by

$$g(\omega) = g_0 \exp[-(\omega-\omega_0)^2/\gamma^2] , \tag{B10}$$

of width (FWHM)

$$W_3 = 2\sqrt{\ln 2}\,\gamma . \tag{B11}$$

There are again simple analytic results in two limiting cases.

(i) $g_0 z \ll 1$. In this case the gain coefficient (3.8) is approximately

$$G(\omega) = 1 + 2g_0 z \exp[-(\omega-\omega_0)^2/\gamma^2] , \tag{B12}$$

and the output flux (3.14) is

$$F_{\text{out}} = G_0 F_{\text{in}} + \frac{\gamma(G_0-1)}{2\sqrt{\pi}} . \tag{B13}$$

The measured intensity fluctuation spectrum (3.20) is

$$\begin{aligned}
S(\omega) = {}& \zeta G_0 F_{\text{in}} + [\zeta\gamma(G_0-1)/2\sqrt{\pi}] \\
& + 2\zeta^2 G_0(G_0-1)F_{\text{in}}\exp(-\omega^2/\gamma^2) \\
& + \frac{\zeta^2}{2}(G_0-1)^2[\gamma/\sqrt{2\pi}]\exp(-\omega^2/2\gamma^2) .
\end{aligned} \tag{B14}$$

(ii) $g_0 z \gg 1$. The high-gain limit of the gain coefficient for the Gaussian variation of the wave vector can be found by the same procedure as used in the Lorentzian case, and indeed the result is identical to that given in (B6). Thus the output flux and intensity fluctuation spectrum are given by (B8) and (B9), respectively.

*Present address: Department of Physics and Applied Physics, University of Strathclyde, John Anderson Building, 107 Rottenrow, Glasgow G4 0NG, United Kingdom.

[1] See, for example, Quantum Measurements in Optics, Proceedings of the 1991 NATO Conference in Cortina, edited by P. Tombesi (Plenum, New York, 1992).

[2] See, for example, R. Loudon, The Quantum Theory of Light (Clarendon, Oxford, 1983).

[3] C. M. Caves and D. D. Crouch, J. Opt. Soc. Am. B 4, 1535 (1987).

[4] N. Imoto (unpublished).

[5] K. J. Blow, R. Loudon, S. J. D. Phoenix, and T. J. Shepherd, Phys. Rev. A 42, 4102 (1990).

[6] I. Abram, Phys. Rev. A 35, 4661 (1987).

[7] T. A. B. Kennedy and E. M. Wright, Phys. Rev. A 38, 212 (1988).

[8] P. D. Drummond, Phys. Rev. A 42, 6845 (1990).

[9] R. J. Glauber and M. Lewenstein, Phys. Rev. A 43, 467 (1991).

[10] I. Abram and E. Cohen, Phys. Rev. A 44, 500 (1991).

[11] P. D. Drummond and M. G. Raymer, Phys. Rev. A 44, 2072 (1991).

[12] B. Huttner, J. J. Baumberg, and S. M. Barnett, Europhys. Lett. 16, 177 (1991).

[13] J. R. Jeffers, R. Loudon, K. J. Blow, and S. J. D. Phoenix, in Nonlinear Dynamics and Quantum Phenomena in Opti-

cal Systems, Proceedings of the 1990 Blanes Conference, edited by R. Vilaseca and R. Corbalan (Springer-Verlag, Berlin, 1992), p. 14.

[14] N. Imoto, J. R. Jeffers, and R. Loudon, in Quantum Measurements in Optics, Proceedings of the 1991 NATO Conference in Cortina, edited by P. Tombesi (Plenum, New York, 1992), p. 295.

[15] D. D. Crouch, Phys. Rev. A 38, 508 (1988); B. Huttner, S. Serulnik, and Y. Ben-Aryeh, ibid. 42, 5594 (1990).

[16] A. Mecozzi and P. Tombesi, Opt. Commun. 75, 256 (1990).

[17] K. Kikuchi, Electron. Lett. 26, 1851 (1990); G. R. Walker, D. M. Spirit, D. L. Williams, and S. T. Davey, ibid. 27, 1390 (1991).

[18] P. R. Battle, R. C. Swanson, and J. L. Carlsten, Phys. Rev. A 44, 1922 (1991).

[19] R. Loudon, in Frontiers in Quantum Optics, edited by E. R. Pike and S. Sarkar (Adam Hilger, Bristol, 1986), p. 42.

[20] G. P. Agrawal, Nonlinear Fiber Optics (Academic, San Diego, 1989).

[21] M. J. Collett, R. Loudon, and C. W. Gardiner, J. Mod. Opt. 34, 881 (1987).

[22] L. D. Landau and E. M. Lifshitz, Statistical Physics (Pergamon, Oxford, 1980), Vol. 1, p. 393.

[23] H. B. Dwight, Tables of Integrals (Macmillan, New York, 1961).

[24] M. J. Collett and R. Loudon, J. Opt. Soc. Am. B **4**, 1525 (1987).

[25] J. D. Cresser, Phys. Scr. **T21**, 52 (1988).

[26] R. J. Glauber, in *Frontiers in Quantum Optics,* edited by E. R. Pike and S. Sarkar (Adam Hilger, Bristol, 1986), p. 534.

[27] C. M. Caves, Phys. Rev. D **26**, 1817 (1982).

[28] R. Loudon and T. J. Shepherd, Opt. Acta **31**, 1234 (1984).

[29] Y. Yamamoto and T. Mukai, Opt. Quant. Electron. **21**, S1

[30] M. Harris, R. Loudon, T. J. Shepherd, and J. M. Vaughan, J. Mod. Opt. **39**, 1195 (1992).

[31] S. Friberg and L. Mandel, Opt. Commun. **46**, 141 (1983).

[32] G. L. Mander, R. Loudon, and T. J. Shepherd, Phys. Rev. A **40**, 5753 (1989).

[33] K. Rzazewski, M. Lewenstein, and M. G. Raymer, Opt. Commun. **43**, 451 (1982).

(1989).